

# Thirty million year deep-sea records in the South China Sea

WANG Pinxian<sup>1</sup>, ZHAO Quanhong<sup>1</sup>, JIAN Zhimin<sup>1</sup>,  
CHENG Xinrong<sup>1</sup>, HUANG Wei<sup>1</sup>, TIAN Jun<sup>1</sup>,  
WANG Jiliang<sup>1</sup>, LI Qianyu<sup>1</sup>, LI Baohua<sup>2</sup> & SU Xin<sup>3</sup>

1. Key Laboratory of Marine Geology, Ministry of Education, Tongji University, Shanghai 200092, China;
2. Nanjing Institute of Geology and Palaeontology, Chinese Academy of Sciences, Nanjing 210008, China
3. Geoscience University of China, Beijing 100083, China

**Abstract** In the spring of 1999 the Ocean Drilling Program (ODP) Leg 184 Shipboard Party cored 17 holes at 6 deep water sites in the northern and southern parts of the South China Sea (SCS). Chinese scientists actively participated in the entire process of this first deep-sea drilling leg off China, from proposal to post-cruise studies. More than 30 categories of analyses have been conducted post-cruise in various Chinese laboratories on a large number of core samples, and the total number of analyses exceeded 60 thousand. The major scientific achievements of the Leg 184 studies are briefly reported in three successive papers, with the first one presented here dealing with deep-sea stratigraphy and evolution of climate cycles. This ODP leg has established the best deep-sea stratigraphic sequences in the Western Pacific: the 23-Ma isotope sequence from the Dong-Sha area is unique worldwide because of its continuity; the last 5-Ma sequence from the Nansha area represents one of the best 4 ODP sites worldwide with the highest time-resolution for that time interval, and the sequences of physical properties enable a decadal-scale time resolution. All these together have provided for the first time high-quality marine records for paleoenvironmental studies in the Asian-Pacific region. This new set of stratigraphic records has revealed changes in climate cyclicality over the last 20 Ma with the fluctuating power of the 100 ka, 400 ka, 2000 ka eccentricity cycles, indicating the evolving response of the climate system to orbital forcing along with the growth of the Antarctic and Northern Hemisphere ice sheets.

**Keywords:** ODP Leg 184, South China Sea, late Cenozoic, climate changes, orbital cycles.

DOI: 10.1360/03wd0154

In the spring of 1999, the international drilling vessel “JOIDES Revolution” entered the South China Sea and completed the Ocean Drilling Program (ODP) Leg 184 with great successes. This was the first deep-sea scientific drilling leg to the seas off China. The operation lasted from February to April and collected a large amount of high-quality sediment cores and data. The drilling and the subsequent over three-year post-cruise studies have promoted the SCS into the international frontier of the deep-sea studies. The contribution of Leg 184 to paleo-

ceanographic and paleoclimatic research in China is both momentous and enduring.

The Deep Sea Drilling Program (DSDP, 1968—1983) and ODP (1985—2003) have been the greatest international cooperation in earth sciences in the 20th century, with nearly 3000 holes drilled and 300 km of cores recovered from the global ocean. The DSDP/ODP have validated the theory of plate tectonics, created the new discipline of paleoceanography, discovered numerous underwater facts including deep-sea biosphere and gas hydrate, and provided an impetus to newer and newer breakthroughs in Earth sciences. The ODP Leg 184 to the SCS was entitled “East Asian monsoon history as recorded in the South China Sea and its global climate impact”, and aimed to recover continuous deep-sea records, to reconstruct the evolution of the climate system, namely the East Asian monsoon system, and to identify its driving forces. The Leg cored 17 holes at 6 deep water sites in the northern and southern parts of the SCS, ranging from ca. 2000 m to 3300 m water depths, with a maximal penetration of 850 m below the sea floor. A total of 55 km of high-quality cores was collected with nearly 95% recovery, over-fulfilling the original target (Figs. 1 and 2; Table 1<sup>[1]</sup>). The hemipelagic sediment sequences recovered by the Leg using advanced techniques provide, for the first time, continuous high-quality marine records over the last 30 Ma for paleoenvironmental studies in the Asian-Pacific region and for better understanding of the SCS basin formation and its mineral resources.

Because of the historical reason, China was unable to participate in international deep-sea scientific drilling activities until 1998, when China joined the ODP as its first “Associate Member”. Noticeable is the drilling leg off China successfully implemented only one year after China’s participation in ODP, which is an extremely rare case in the DSDP/ODP history. The ODP Leg 184 was proposed and designed by Chinese scientists, with a Chinese Co-Chief Scientist and several other Chinese marine geologists on board. After the cruise, eight laboratories from 5 cities joined the project supported by the National Natural Science of China to analyze the core samples from the leg. In result, more than 30 categories of analyses were conducted on a large number of core samples in these Chinese laboratories, with the total number of analyses exceeding 60 thousand, including tens of thousands of isotopic and micropaleontological analyses (Table 2).

In general, the ODP Leg 184 to the SCS recovered deep-sea sediment sequences that recorded the past 32 Ma environmental history of the SCS, established the best deep-sea stratigraphic sequences for the Western Pacific, and for the first time explored the evolution of climate cyclicality over the last 20 Ma in the region. The Leg also discovered long-term periodicities in oceanic carbon cycling, and demonstrated the role of tropical forcing in the evolution of climate cycles. These results helped promote

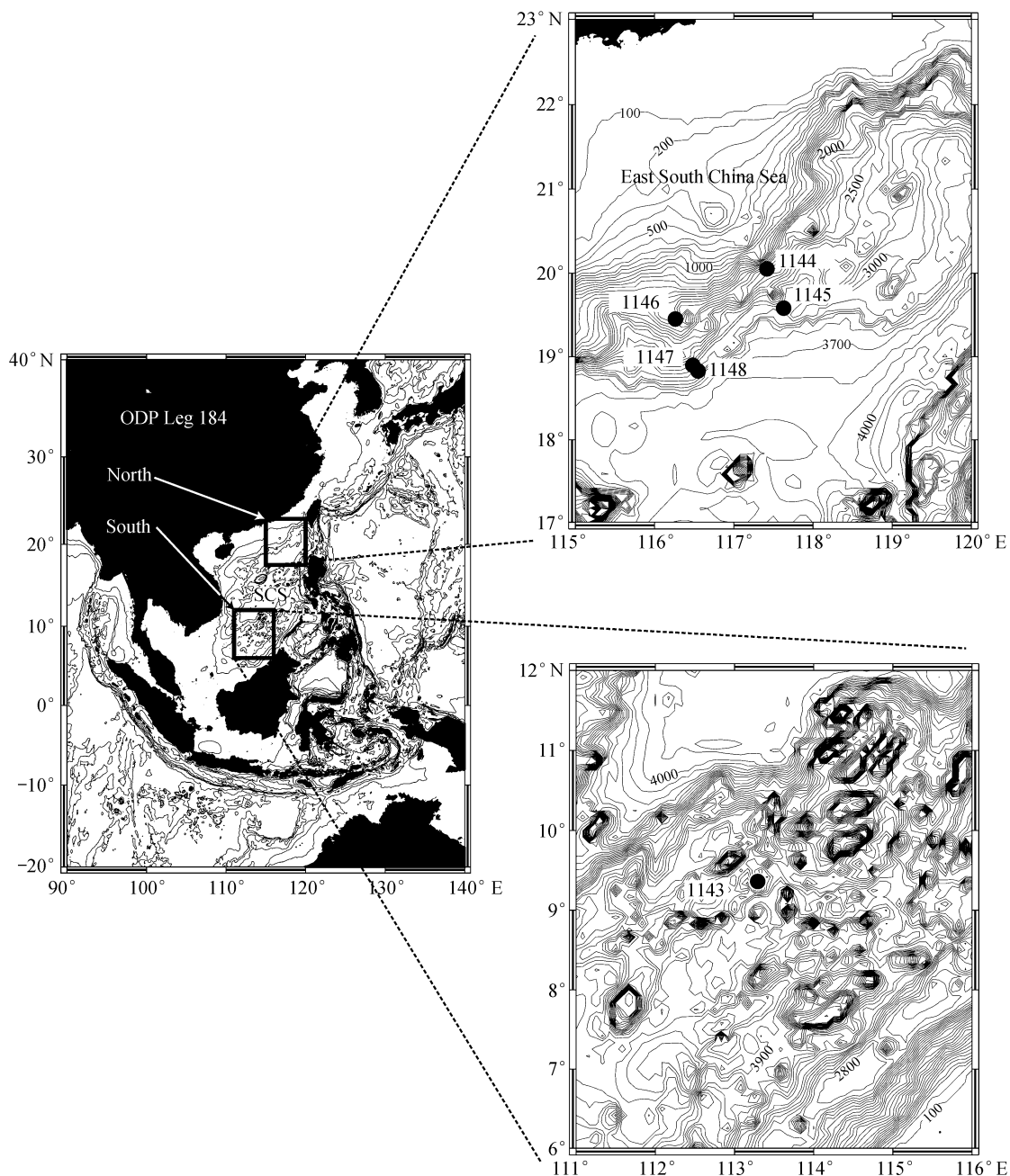


Fig. 1. Location map of ODP Leg 184 sites in the South China Sea<sup>[1]</sup>.

Table 1 Summary of Leg 184 sites cored in the South China Sea

Area	Site	Latitude/longitude	Water depth/m	Penetration/m	Holes	Age at base/Ma	Core length/m
Nansha	1143	9°22'N/113°17'E	2272	500	3	~11	1100
	1144	20°03'N/117°25'E	2037	450	3	~1	1110
	1145	19°35'N/117°38'E	3175	200	3	~3	555
Dongsha	1146	19°27'N/116°16'E	2092	600	3	~19	1450
	1147	18°50'N/116°33'E	3246	80	3	~1.4	240
	1148	18°50'N/116°34'E	3294	850	2	~32	1000

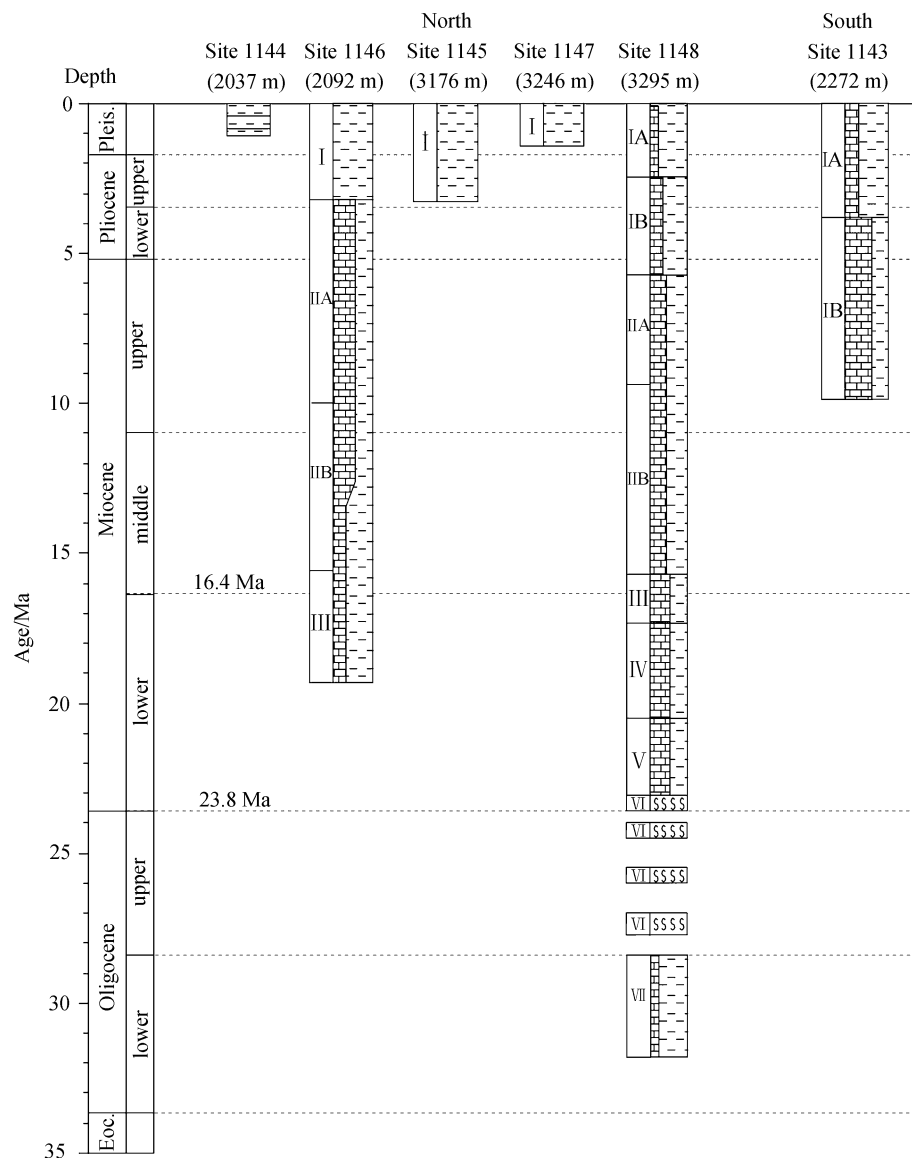


Fig. 2. Summary of coring penetration and lithological units at Leg 184 drilling sites, South China Sea<sup>[1]</sup>.

Table 2 Analyses of ODP 184 samples performed in laboratories in China

Analytic category	Number of samples
Oxygen and carbon isotopes	15036
Micropaleontology	23026
Pollen and spores	2320
Geochemistry	9225
Mineralogy, granulometry, coarse fraction	7562
Others	9305
Total	66474

a concept of climate changes likely controlled by a combination of low- and high-latitude forcing, of hydrological

and carbon cycling, and superimposed by long and short astronomical cyclicities. A multi-proxy approach applied to the deep-sea records for reconstructing the East Asian monsoon history has revealed its step-wise evolution very similar to the Indian monsoon, with the major difference being the strength of winter monsoon in East Asia. The spectrum of the monsoon variations in the southern part of the SCS consistently displayed a remarkable low-latitude feature.

Another major achievement was sedimentary evidence for the basin evolution of the SCS. The discovery of deep-sea Oligocene deposits implied the existence of a deep-sea environment already at the beginning of the sea-floor spreading of the SCS basin over 32 Ma ago in the very early period of the early Oligocene, followed by

the most intensive tectonic deformation in the late Oligocene. The conspicuous North-South contrast in the modern SCS environmental settings first appeared about 3 Ma ago. The drilling of Leg 184 and post-cruise investigations has greatly strengthened land-sea linkage in Earth sciences studies and promoted the deep-sea researches in China into the international frontiers.

The present paper is the first of three brief summary reports of the Chinese studies on ODP Leg 184, dealing mainly with the deep-sea stratigraphy and evolution of climate cycles. The results of long-term oceanic carbon cycles, and the evolution of the monsoon system and the SCS basin will be discussed in the second and third reports, respectively. Since all the three papers are mainly based on papers in press or in review, the reader is referred to those papers for more precise and detailed information.

### 1 30 Ma deep-sea record

The late Cenozoic is the best studied section of the Earth history in terms of the global climate changes, but China's contribution is hindered by its lack of marine deposits of that time interval on its mainland. The basic contribution of Leg 184 is the recovery of continuous deep-sea deposits for the last 32 Ma and a complete late Cenozoic stratigraphic sequence which made high-resolution paleoenvironmental reconstruction possible for the region.

Complete sediment records for various time intervals with different resolution are available from Leg 184 sites (Figs. 2 and 3); and the new techniques used by ODP<sup>[1]</sup> facilitated a high quality of the cores recovered.

The longest sediment section of Leg 184 was cored at Site 1148 on the lowermost northern slope (water depth about 3300 m) near the Dongsha Island, with the 850 m section representing a 32 Ma record. A total of 1580 samples from its upper 457 m were analyzed for foraminifers and stable isotopes, and the combined results of bio- and magneto-stratigraphies helped establish a continuous 23.7 Ma sequence for the entire Neogene with an average sampling interval of 16 ka (Fig. 3(a); for preliminary reports see<sup>[2,3]</sup>). This is the most continuous and high-resolution Neogene deep-sea sequence from the Western Pacific, and also the only late Cenozoic isotopic sequence in the global ocean from a single site. At Site 1143 (water depth 2772 m) from the Nansha area, the only site from the southern SCS, foraminifers and isotopes were analyzed in 1800 samples from the upper 200-m section, resulting in a 5-Ma sequence with an average sampling interval of 2–3 ka. After astronomical tuning, the Site 1143 sequence provides a first high-resolution, 5-Ma long record for the Western Pacific and one of the best such records from the global ocean (Fig. 3(b)<sup>[4]</sup>; for preliminary results see [5]). Site 1144 is located on a

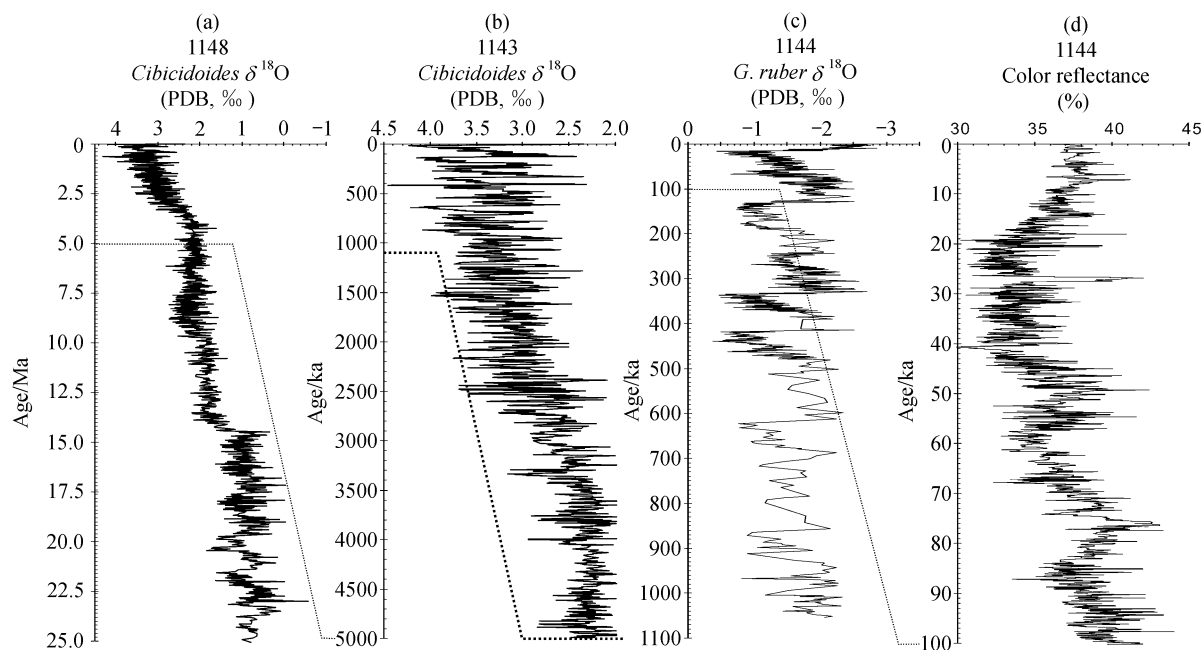


Fig. 3. High-resolution stratigraphic sequences established by the ODP Leg 184 studies. (a) 23 Ma record of benthic  $\delta^{18}\text{O}$  at Site 1148 with average sampling interval of 16 ka (provided by Zhao and others); (b) 5 Ma record of benthic  $\delta^{18}\text{O}$  at Site 1143 with average sampling interval of 2.6–2.8 ka<sup>[4]</sup>; (c) 1 Ma record of planktonic  $\delta^{18}\text{O}$  at Site 1144 with average sampling interval of 900 years (Buehring et al.<sup>[1]</sup>); (d) 0.1 Ma record of colour reflectance at Site 1144 with average sampling interval of about 60 years<sup>[1]</sup>. All isotopic analyses were performed in the Key Laboratory of Marine Geology, Tongji University, except for Site 1144.

1) Buehring, C. et al., Toward a high-resolution stable isotope stratigraphy of the last 1.1 million years: Site 1144, South China Sea, ODP Scientific Results, 184, in press.

sediment draft on the middle continental slope southeast of the Dongsha Island<sup>[6]</sup>, with the >500 m sediment sequence recovered representing the past 1 Ma. Oxygen and carbon isotope analyses at site 1144 were performed at the Kiel University, Germany, providing an average high-resolution of nearly 900 years (Fig. 3(c); Buehring et al.<sup>[1]</sup>). Recent studies by W. Huang et al. indicate that the colour reflectance record can be used as a proxy of CaCO<sub>3</sub>% at Site 1144, and the colour reflectance curve measuring 2 cm apart represents a carbonate record with decadal resolution (Fig. 3(d)). In sum, Leg 184 has provided high-resolution deep-sea records of late Cenozoic environmental changes at various time scales, ranging from 10<sup>4</sup> years (Site 1148), 10<sup>3</sup> years (Site 1143), to 10<sup>2</sup> and 10<sup>1</sup> years (Site 1144).

Although only oxygen-isotopic and colour reflectance records are shown in Fig. 3, the stratigraphy at all Leg 184 sites is based first of all on biostratigraphic (foraminifers, calcareous nannofossils, radiolarians, diatoms, dinoflagellates, pollen and spores) and magnetostratigraphic data. Aside from the preliminary ship-board results<sup>[1]</sup>, a series of micropaleontological analyses have been done in Chinese laboratories (of those only a small part has been published such as [7]). Over 80 nannofossil and foraminiferal datums were identified (Table 3) for the last 5 Ma at Site 1143 and for earlier time periods at Site 1148. A combination of biostratigraphy and isotopic stratigraphy has strengthened more accurate correlation of the late Cenozoic sequence in the SCS.

In order to evaluate the significance of the newly established deep-sea sequences in the SCS, stratigraphic and isotopic sequences from other oceans were compared. A literature search has found only three other sites with isotopic records longer than 5 Ma with time resolution on the thousand year scale: ODP Sites 846 and 849 from the Eastern Pacific, and ODP Site 659 from the North Atlantic (Table 4, Fig. 4). Therefore, Site 1143 is the first in the Western Pacific, and the only site in the global ocean providing such long and continuous benthic and planktonic records. Among sites with isotope sequences of 20 Ma or longer, three have a time resolution of 10<sup>4</sup> years: DSDP Sites 588 and 590 from the Southwest Pacific and ODP Site 709 from the Indian Ocean, and four have a time resolution of 10<sup>5</sup> years: DSDP 289 from the Northwest Pacific, DSDP 563 and 608 from the Atlantic, and ODP 747 from the Southern Ocean (Table 4; Fig. 4). At all the above-mentioned sites, however, the record is neither continuous nor complete because sections from the past 2 to 8 Ma are missing. Therefore, the Site 1148 record is unique worldwide in providing a continuous record for the entire Neogene, from the earliest Miocene to Holocene.

Zachos et al. compiled data from more than 40 DSDP and ODP sites and established global deep-sea

oxygen and carbon isotope records<sup>[19]</sup>, but the smoothed curve based on average values can reflect only the general trend. By contrast, our long record is based on one single site (Site 1148), and thus is more advantageous to provide a precise time sequence for studies of environmental events and changes in climate cyclicality.

## 2 Palaeoenvironmental events

The global climate gradually cooled since the formation of major Antarctic continental ice-sheets at ~36 Ma. Following a series of significant rebounds in the Miocene and early Pliocene, the global climate finally entered the icehouse regime with both poles ice-caped in the late Pliocene and Pleistocene<sup>[19]</sup>. The process of climate evolution over the past 24 Ma can be read from the oxygen and carbon isotopes at Site 1148 (Fig. 5; for preliminary reports see [2, 3]). The oxygen isotope recorded the expansion of the Antarctic ice-sheets in the Miocene, the formation of the Arctic ice-sheets in the late Pliocene, and a number of cooling events; the carbon isotope recorded the global carbon excursions in the Miocene, as well as some regional events in the late Miocene and Pliocene.

(i) Cooling events since the Miocene. Just as in other sea areas, the benthic foraminiferal oxygen isotope at Site 1148 has recorded a series of global cooling events in the late Cenozoic (Fig. 5(a)), and the most prominent were the <sup>18</sup>O-rich events in the early middle Miocene (14.2—13.6 Ma) and in the late Pliocene (3.5—2.5 Ma) when the  $\delta^{18}\text{O}$  value increased by 0.94‰ and 0.99‰, respectively. The former event indicates the most pronounced expansion of ice-cap on Antarctic leading to its permanent existence, the significant cooling of the bottom water and the establishment of the modern pattern of bottom water circulation<sup>[17,18,20]</sup>; the latter is related to the formation of the Arctic ice-sheets in the late Pliocene and the transition of the Earth system from “one-polar ice-caped” to “two-polar ice-caped”, entering into the glacial climate regime<sup>[19]</sup>. Besides, there is a series of cooling events in the Miocene record, as seen from the heavy values of  $\delta^{18}\text{O}$  at 23.2, 21.7, 20.0, 17.8, 16.0, 14.2, 13.6, 11.2, and 9.6 Ma, corresponding to Mi1.1, Mi1a, Mi1aa, Mi1b, Mi2, Mi3a, Mi3b, Mi4, Mi5 and Mi6 events<sup>[17,21,22]</sup>. One more  $\delta^{18}\text{O}$  increase to a similar large amplitude happened at 0.9 Ma after the late-Pliocene formation of the Arctic ice-sheets, reflecting the further growth of the boreal ice-cap<sup>[23,24]</sup>.

(ii) Early Pliocene warming event. The planktonic foraminiferal  $\delta^{18}\text{O}$  at Site 1148 becomes remarkably light in the Pliocene between 5.2 and 3.2 Ma (Fig. 5(a)). Especially during the 5.2—4.2 Ma interval, the negative  $\delta^{18}\text{O}$  spikes are 0.3‰—0.8‰ lighter than the modern value, implying the warmest time period since the later part of the middle Miocene after 14 Ma, and the sea surface tem-

1) See footnote 1) on page 2527.

Table 3 Late Cenozoic planktonic foraminiferal and nannofossil datums, based on Site 1143 for the last 5 Ma, and Site 1148 for earlier sections<sup>a)</sup>

Site	Foraminiferal datums	Depth /mcd	Age/Ma	Nannofossil datums <sup>b)</sup>	Depth/mcd	Age/Ma
1143	LO pink <i>G. ruber</i>	8.07	0.124	FO <i>E. huxleyi</i> Acme	8.04	0.09
	FO pink <i>G. ruber</i>	25.03	0.407	FO <i>E. huxleyi</i>	14.91	0.26
	LO <i>G. fistulosus</i>	83.40	1.729	LO <i>P. lacunosa</i>	26.265	0.46
	FO <i>G. truncatulinoides</i>	96.09	2.031	LO small <i>Gephyrocapsa</i> Acme	52.32	1.02
	LO <i>G. multicamerata</i>	134.71	3.038	LO <i>C. macintyreii</i>	73.845	1.67
	LO <i>D. altispira</i>	134.81	3.041	FO median <i>Gephyrocapsa</i> spp.	93.895	1.73
	LO <i>S. seminulina</i>	138.01	3.138	LO <i>D. brouweri</i>	93.895	1.95
	FO <i>S. dehiscens</i>	158.35	3.800	LO <i>D. pentaradiatus</i>	110.49	2.45
	LO <i>G. tosaensis</i>	144.39	3.348	LO <i>D. surculus</i>	120.45	2.52
	LO <i>G. plesiotumida</i>	161.05	3.823	LO <i>Sphenolithus abies/neoabies</i>	152.72	3.66
	LO <i>G. margaritae</i>	161.58	3.833	LO <i>R. pseudoumbilicus</i>	160.58	3.75
	<i>Pulleniatina</i> (S toD change)	166.55	4.051	LO <i>A. triconiculus</i>	186.58	4.00
	LCO <i>G. margaritae</i>	166.45	4.047	FCO <i>D. asymmetricus</i>	195.42	4.20
	LO <i>G. nepenthes</i>	176.32	4.586	LO <i>C. acutus</i>	195.68	5.05
	LO <i>S. kochi</i>	185.78	4.887			
1148	FO <i>S. dehiscens</i>	188.16	5.54	FO <i>C. rugosus</i>	187.37	5.23
	FO <i>G. tumida</i>	196.08	5.82	LO <i>T. rugosus</i>	190.37	5.34
	FO <i>G. conglobatus</i>	206.79	6.20	FO <i>C. acutus</i>	190.37	5.37
	FO <i>G. extremus</i>	244.26	8.30	LO <i>D. quinqueringus</i>	193.31	5.54
	LO <i>G. dehiscens</i>	257.16	9.80	LO <i>A. amplificus</i>	198.57	5.99
	FO <i>N. acostaensis</i>	259.70	9.82	FO <i>A. amplificus</i>	211.27	6.76
	LO <i>G. mayeri</i>	275.22	10.49	FO <i>A. primus</i>	219.37	7.24
	FO <i>G. nepenthes</i>	283.78	11.19	FO <i>D. berggrenii</i>	242.61	8.20
	LO <i>G. fohsi</i>	301.02	13.00	FO <i>D. quinqueringus</i>	242.61	8.28
	FO <i>G. fohsi</i>	303.28	13.42	FO <i>D. pentaradiatus</i>	253.37	8.55
	FO <i>G. praefohsi</i>	308.68	14.00	LO <i>D. hamatus</i>	256.37	9.40
	LO <i>P. glomerosa</i>	312.38	14.80	LO <i>C. calyculus</i>	261.81	9.64
	FO <i>G. praemenardii</i>	317.98	14.90	LO <i>C. coalithus</i>	267.47	9.69
	LO <i>G. insueta</i>	320.97	15.00	FO <i>D. hamatus</i>	275.57	10.38
	FO <i>Orbulina</i>	320.37	15.10	FO <i>C. calyculus</i>	279.21	10.70
	FO <i>P. glomerosa</i>	344.18	16.10	FO <i>C. coalithus</i>	281.01	10.79
	FO <i>P. curva</i>	352.98	16.30	LO <i>D. kugleri</i>	286.67	11.80
	FO <i>P. sicana</i>	355.39	16.40	FO <i>D. kugleri</i>	293.27	12.20
	LO <i>C. dissimilis</i>	364.88	17.30	FO <i>T. rugosus</i>	302.87	13.20
	FO <i>G. praescitula</i>	379.53	18.50	LO <i>C. floridanus</i>	302.87	13.20
	FO <i>G. insueta</i>	367.37	18.00	LO <i>S. heteromorphus</i>	308.81	13.57
	LO <i>G. binaiensis</i>	377.18	19.10	LO <i>H. ampliapertura</i>	331.87	15.60
	FO <i>G. altiapertura</i>	406.38	20.50	FO <i>S. heteromorphus</i>	370.17	18.20
	LO <i>P. kugleri</i>	408.83	21.50	LO <i>S. belemnus</i>	371.57	18.30
	FO <i>G. dehiscens</i>	454.17	23.20	FO <i>S. belemnus</i>	390.97	19.20
	FO <i>P. kugleri</i>	460.12	23.80	FO <i>D. druggii</i>	454.41	23.20
	FO <i>P. pseudokugleri</i>	475.77	25.90	LO <i>S. capricornutus</i>	458.57	23.70
	LO <i>P. opima</i>	478.52	27.10	LO <i>S. delphix</i>	458.57	23.80
	LO <i>C. cubensis</i>	487.77	28.50	LO <i>R. bisectus</i>	461.57	23.90
	FO <i>G. angulisuturalis</i>	601.66	29.40	LO <i>Z. bijugatus</i>	468.92	24.50
LO <i>T. ampliapertura</i>	634.46	30.30	LO <i>S. ciproensis</i>	473.61	25.50	
FO <i>P. opima</i>	663.32	30.60	LO <i>S. distentus</i>	485.34	27.50	
			FO <i>S. ciproensis</i>	620.99	29.90	
			FO <i>S. distentus</i>	673.41	31.50	
			LO <i>R. umbilicus/R. hillae</i>	730.33	32.30	

a) LO, Last occurrence; FO, first occurrence; LCO, last common occurrence; FCO, first common occurrence; Acme, acme zone; b) nannofossil datums at Site 1143 according to [1].

Table 4 Comparison of high-resolution long-term oxygen isotope sections in various oceans<sup>a)</sup>

Ocean	Site	Latitude & longitude	Water depth /m	Age/Ma	Isotope	Average resolution/ka	Reference
Last 5 Ma							
West Pacific	1143	9°22'N	2772	0—5	benthic	2.8	[4]
		113°17'E				2.6	
East Pacific	846	3°06'S	3296	0—6	benthic	2.5	[8]
		90°49'W					
	849	0°11'N	3851	0—5	planktonic	~4	[9]
		110°31'W					
North Atlantic	659	18°05'N 21°02'W	3070	0—5	benthic	~4	[10]
Last 20 Ma							
West Pacific	1148	18°50.17'N	3294	0—24	benthic	16	new
		116°94'E				21	
	289	0°30'S	2206	5—21	benthic	53	[11—13]
		158°31'E					
	588	26°07'S 161°14'E	1533	4—24	benthic	37	[14, 15]
590	31°10'S 163°22'E	1299	2—20	benthic planktonic	85 72	[14]	
Indian	709	3°55'S 60°33'E	3041	5—25	benthic	90	[16]
Atlantic	563	33°39'N 43°46'W	3786	8—26	benthic	108	[17, 18]
Southern	747	54°49'S 76°48'E	1695	8—25	benthic	97	

a) Included only sequences of 5 Ma or longer with  $10^3$  years resolution, and sequences of 20 Ma or longer with  $10^4$  years resolution (no more than 110 ka).

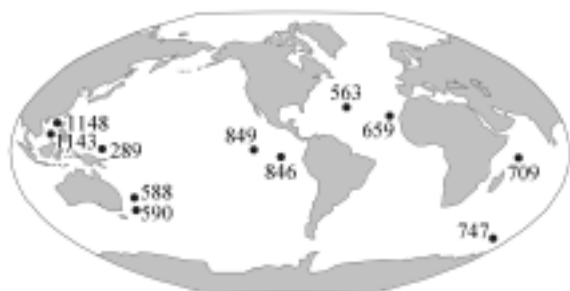


Fig. 4. Distribution of high-resolution long-range isotopic sequences in the global ocean (see Table 4).

perature (SST) warming was calculated as about 1—3°C higher than the modern value. There was, by contrast, no pronounced change in the benthic  $\delta^{18}\text{O}$  record, probably indicating that major ice-melting on Antarctic associated with the early Pliocene warm was weak or absent<sup>[25]</sup>.

(iii) Positive Carbon Excursion in Miocene. The earliest Neogene  $\delta^{13}\text{C}$  positive excursion is known as the carbon isotope maxima at the Oligocene/Miocene boundary (the CM-O/M event) lasting from the end of the Oligocene to ~22.6 Ma<sup>[22,26,27]</sup>, followed by a declining stage of  $\delta^{13}\text{C}$ . Despite of the incomplete stratigraphic record of the latest Oligocene at 1148, the  $\delta^{13}\text{C}$  decrease until 22.3 Ma is well recognizable. The Monterey carbon excursion<sup>[28]</sup> between the early and middle Miocene is outstandingly exhibited at 1148 and reflects the fractionation between the Atlantic and Pacific oceans and the accumulation of diatom-rich deposits in the Pacific rim. As seen from Fig. 5(b), the benthic  $\delta^{13}\text{C}$  at Site 1148 increased

since 17.8 Ma, reached the maximum at 16.0 Ma, then gradually decreased until 13.2 Ma. Noticeable is the relationship between the carbon cycling and ice sheets: both the positive excursion events are followed by ice-sheet expansion as expressed by the  $\delta^{18}\text{O}$  increases, namely the Mi1a and Mi3a,b events<sup>[3]</sup>.

(iv) Negative Carbon Excursions in Late Miocene. The  $\delta^{13}\text{C}$  negative excursion between 10.2—9.6 Ma was recorded in the benthic curve, 1.2‰ lighter than the Miocene average, but not in the planktonic record. As the  $\delta^{13}\text{C}$  excursion led the  $\delta^{18}\text{O}$  maximum event of Mi6 by some 100 ka and was reported also from DSDP Sites 289 and 588 in the Pacific, it is suggested to be related to a significant narrowing or temporary closure of the Central American passageway at 10—9.5 Ma and the development of the Antarctic Bottom Water<sup>[29]</sup>, demonstrating that the changes in carbon reservoir led those in ice-sheets in the Earth system. The Messinian carbon shift<sup>[26,28]</sup> at the end of Miocene, or the Chron 6 carbon shift<sup>[28]</sup>, is a widely reported global event with the well-known Mediterranean desiccation event as its follow-up. This is recorded at Site 1148 as a large amplitude decrease in benthic and planktonic  $\delta^{13}\text{C}$  between 6.9 and 6.2 Ma (Fig. 5(b)).

(v) Negative carbon excursions in latest Pliocene and Pleistocene. There are also regional or local events in the SCS record. Thus, the planktonic  $\delta^{13}\text{C}$  at Site 1148 sharply decreased at the Plio-Pleistocene turn (2.3—1.6 Ma), with minimal values by 1.1‰ lighter than the modern, but no significant change in the benthic  $\delta^{13}\text{C}$  record. This must be a regional carbon shift caused likely by the

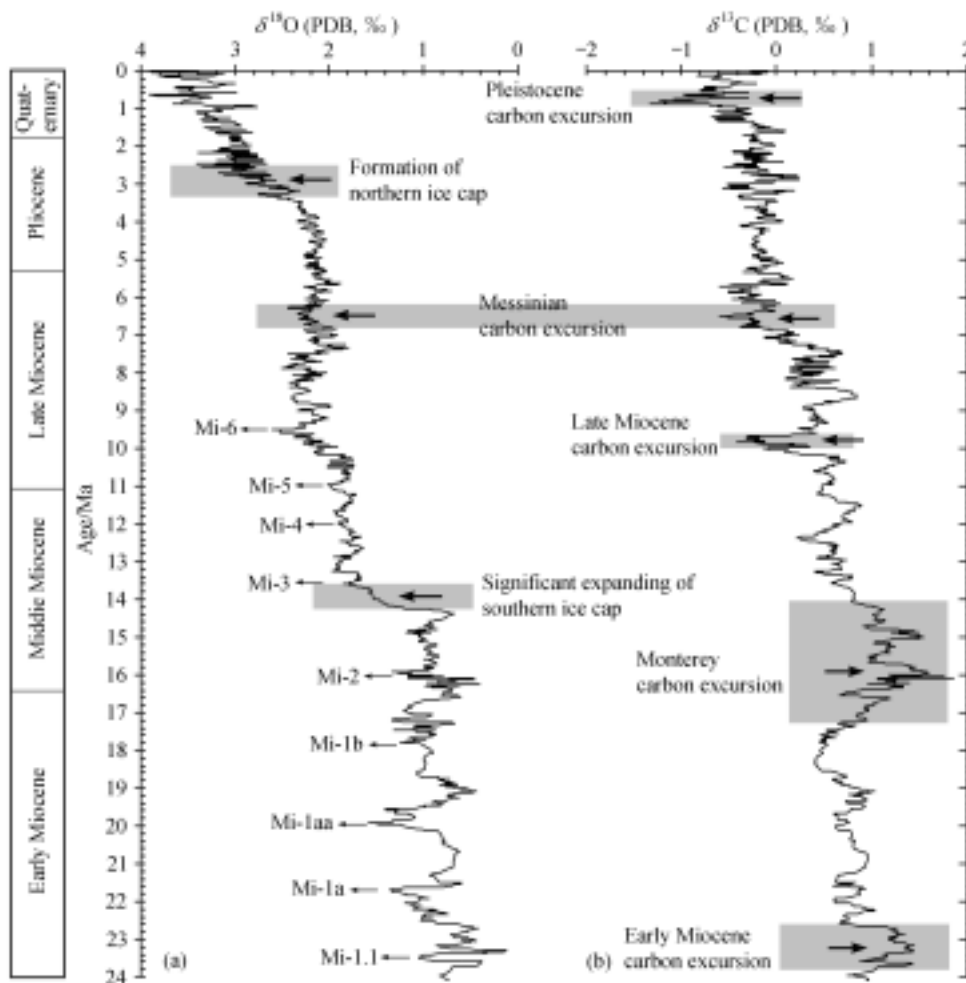


Fig. 5. Major environmental events recorded in isotopic sequences at Site 1148 since the Miocene (such as Mi1.1, see the text for details). (a) Benthic oxygen isotope; (b) benthic carbon isotope. All curves are 5-point smoothed.

enhanced surface productivity as a result of the intensified Asian winter monsoon<sup>[23,24]</sup>. Later, a drastic negative excursion of benthic  $\delta^{13}\text{C}$  occurred at Site 1148 in the middle Pleistocene, between 1.0 and 0.4 Ma (Fig. 5(b)), supposedly recording some changes of bottom water in the SCS due to the rise of the Bashi Strait, the sill separating the SCS from the Pacific.

### 3 Climate cyclicity and its evolution

The Earth history is nothing but a combination of events and cycles, and the most typical cycles are those in the Quaternary glaciation which have been deciphered by the Milankovitch theory of orbital forcing. The ODP Leg to the SCS for the first time provided us with a wealth of deep-sea data for studies on orbital cycles at various timescales.

Because the glaciation during the last tens of thousand years displays prevalently a 100 ka periodicity, the transition from the predominantly 40 ka oscillations to the 100 ka cycles has attracted particular attention in the sci-

entific circles. This “turnover” in climate changes at about 0.9 Ma was described as the “Mid-Pleistocene Revolution”<sup>[30]</sup>, though this “revolution” was transitional in nature as recorded in the SCS at Site 1143<sup>[31]</sup>, and similar transitions are observed throughout the late Cenozoic. In fact, the waxing and waning of various orbital cycles have been recorded in the  $\delta^{18}\text{O}$  sequence at Site 1143 over the past 5 Ma: The 40 ka cycle in benthic  $\delta^{18}\text{O}$  has been prominent since the beginning of the section, but strengthened significantly after 2.7 Ma; the 100 ka component is best manifested since 0.9 Ma, but its enhancement started already at 1.5 Ma. Even earlier, in the 2.0 to 3.3 Ma interval, the 100 ka cycle in benthic  $\delta^{18}\text{O}$  already strengthened its amplitude, and this is not unique to Site 1143, as similar observations can be found in the Eastern Pacific and North Atlantic as well (Fig. 6<sup>[4]</sup>), indicating evolutionary changes of the global climate system.

Essentially, the transition to 100-ka cycle was associated with postponement of ice melting in the Arctic: ice sheets did not melt at the end of 40-ka cycle but continued

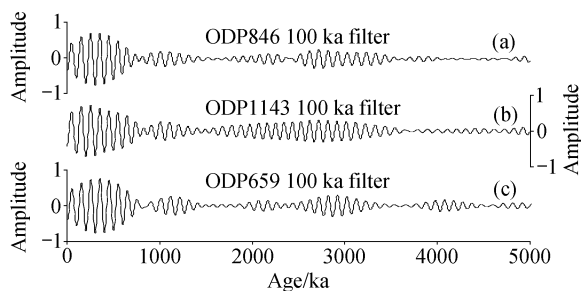


Fig. 6. Bandpass filters of the 5-Ma benthic oxygen isotope records of three ODP sites at 100-ka band. (a) Site 846, East Pacific; (b) Site 1143, West Pacific; (c) Site 659, North Atlantic.

to grow over 100-ka, resulting in the “Mid-Pleistocene Revolution”. More accurately, the late Quaternary “100-ka” glacial cycles are in fact mostly 80- or 120-ka, or four to six precessional cycles long, and real 100-ka cycles are rare<sup>[31]</sup>. An earlier sign of glacial cycle extension is exemplified by the unusually long marine isotope stage (MIS) 34 at 1150 ka, which was considered as a “premature”, near-100 ka cycle or an “unsuccessful attempt” of the climate transition<sup>[32,33]</sup>. As shown in Fig. 6, the 100-ka periodicity appeared as early as at 1.4–1.5 Ma<sup>[34]</sup>, and this is the argument of the opinion that the time interval 1.4–0.8 Ma belongs to an “Interim State” of the climate transition<sup>[33]</sup>. Of the Earth’s orbital parameters, the eccentricity varies at the periods of 100 ka and 400 ka and enters the climate system by modulating the amplitude of the precessional cycle; therefore, the 100-ka cycle can be found in the oxygen isotope records over 5 Ma<sup>[35]</sup>, but with a varying intensity. For example, the 100-ka periodicity was strengthened at around 2.5 Ma on the Ontong-Java Plateau<sup>[30]</sup>, Western Pacific, which is in agreement with the SCS record.

The picture becomes even more clear if our scope is broadened to the longer geological past. As seen from the results of low-pass filtering of the 24-Ma benthic record at Site 1148 (Fig. 7(a)), the long-term eccentricity cycles of 100 ka (Fig. 7(b)) and 400 ka (Fig. 7(c)) are observable throughout the Neogene, but the amplitudes vary significantly. The recent studies show that these two periodicities are predominant in the pre-Quaternary deep-sea records<sup>[19]</sup>, and they are best displayed at the Oligocene/Miocene turn after the sequence between 20.5–25.4 Ma was astronomically tuned<sup>[36,37]</sup>. The 100-ka and 400-ka cycles are also well recorded in the middle Miocene (14–16 Ma)<sup>[15]</sup> and late Miocene (12–10 Ma)<sup>[38]</sup> deposits. Moreover, these astronomical periodicities have been widely adopted in the establishment of international stratotypes for the late Miocene and Pliocene<sup>[39]</sup>. Noteworthy are the 2-Ma cycles pronouncedly exhibited in the Site 1148 record (Fig. 7(d)), particularly clear in the sections before 14 Ma and after 5 Ma. The 2-Ma cycle belongs also to eccentricity and modulates the amplitude of the 100- and 400-ka cycles. This long-term eccentricity periodicity was re-

cently reported from the late Miocene  $\delta^{18}\text{O}$  sequence in the Mediterranean<sup>[38]</sup>, but can be hardly detected in other sequences because of the limited length of record. The advantage of high-resolution long records has enabled the ODP Leg 184 studies to discover million-year-long cyclicity. From a marginal sea location that provided an amplifying effect, these records make the amplitude of climate changes much more significant than those from the open ocean, as seen in the much larger  $\delta^{18}\text{O}$  amplitudes in 2-Ma cycle fluctuations (Figs. 5(a), 7(d)).

In sum, the orbital cycles always exist whenever the Earth is rotating, and the climate is always under their influence. However, the influence changes with the geographical location and with the regime of the Earth system. The low latitudes are mainly influenced by the 20-ka precessional cycles, whereas the high latitudes by the 40-ka cycles of obliquity, respectively characterizing the tropical forcing and glacial forcing of the climate system<sup>[40]</sup>. The climate cycles in the ice-free “Hot-house” Earth are mainly driven by the low-latitude precessional forcing with 20-ka cyclicity, which in turn is modulated by eccentricity. The precessional forcing enhances when eccentricity is maximal, and weakens when eccentricity is minimal. Since the tropical region is not sensitive to the low temperature part of the cycle, the “clipping” effect in eccentricity modulated precessional cycle results in a significant response at the modulating frequencies, namely the 100-ka and 400-ka cycles<sup>[41]</sup>. Therefore, the 400-ka eccentricity was the most prominent climate cycle in the “Hot-House” Mesozoic<sup>[42,43]</sup>. In the late Cenozoic, the obliquity cycle became progressively predominant in the glacial variations with the growth of the Antarctic ice-sheets, and the eccentricity cycles retained with varying power in the forcing. The 100-ka cycles enhanced for certain time interval when the boreal ice-sheets started to grow at 3.3 Ma, but weakened toward 2.0 Ma and reappeared at 1.5 Ma (Fig. 6). All these demonstrate the frequency of climate cycle transition in the geological history.

Due to the rarity of high-resolution long-term records in the world, and due to the focus of the climate cycle studies on the late Quaternary, our understanding of the orbital cycles has been strongly biased. The changes of orbital cyclicity in climate become much more comprehensible when the Cenozoic long sequence is investigated in a descending order. It turns out that the Quaternary with ice cap on both poles represents an unusual scenario of the Earth system. The boundary conditions of the climate system were subjected to fundamental reorganization in the evolving process from the ice-free “Hot-House” tens of million years ago, to the “Ice-House” with one, then two poles ice-caped, and the climate system changed its way of response to the orbital cycles. Studies on long sequences are necessary, if we are to find out the mechanism of transition in climate system and to resolve the problems in Quaternary glacial cyclicity<sup>[44]</sup>. The ODP Leg 184 to the

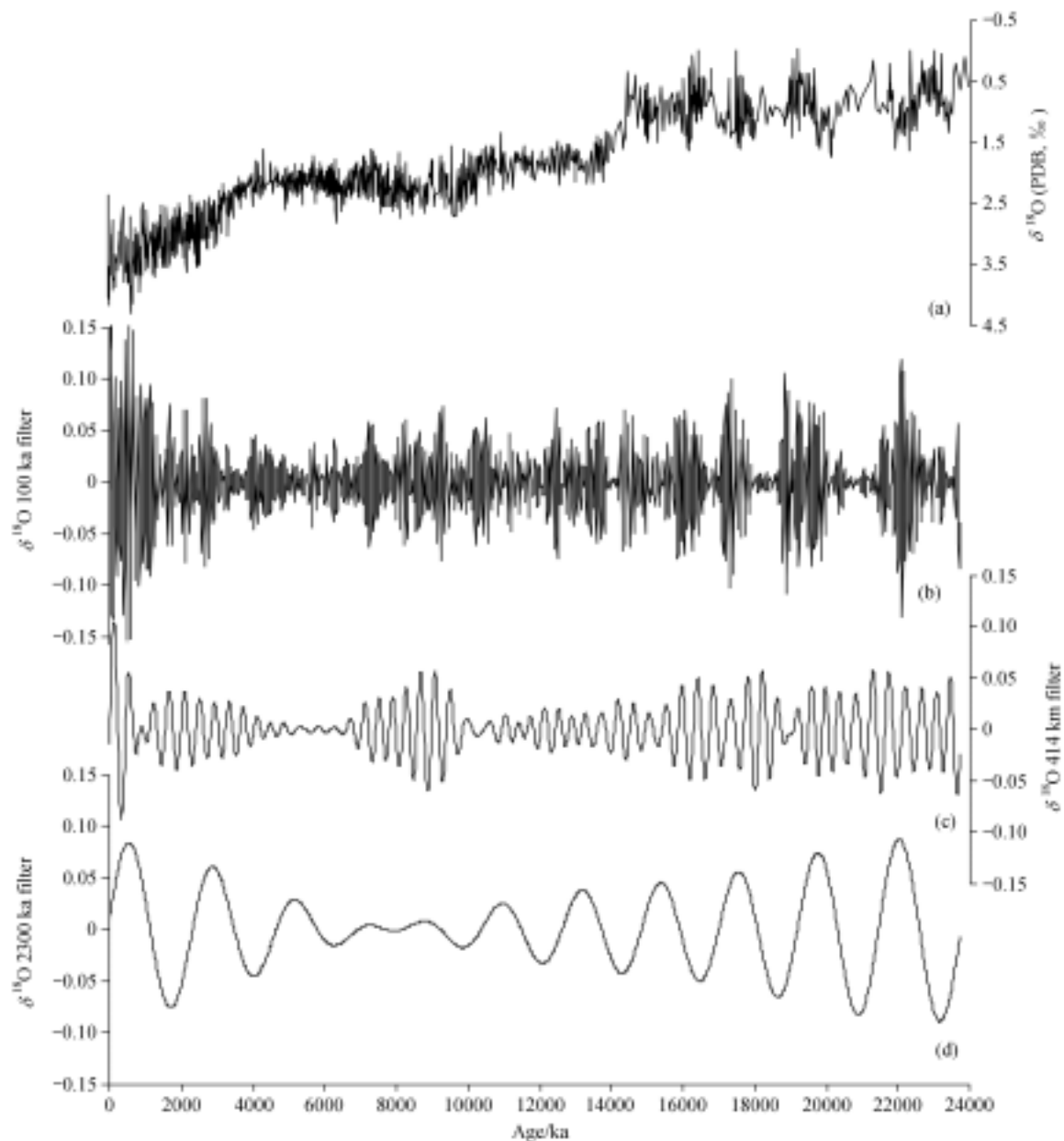


Fig. 7. A 23-Ma benthic isotope record of Site 1148 and its bandpass filters at 100-, 400-, and 2000-ka bands. (a) Benthic  $\delta^{18}\text{O}$ ; (b) 100-ka band; (c) 400-ka band; (d) 2000-ka band.

SCS provided us with such an opportunity. In the next paper (“Evolution of the South China Sea and Monsoon History: Evidence from Deep Sea”) we will show that the  $\delta^{18}\text{O}$  and  $\delta^{13}\text{C}$  co-varied until the formation of the boreal ice cap, but de-coupled afterwards, indicating that the Earth system with two poles covered by ice-sheets is much more complicated than the ice-free or one pole ice-caped Earth.

#### 4 Concluding remarks

The first ocean drilling leg to the China Seas, ODP

Leg 184, was crowned with success, and its great scientific achievements opened up a new phase in paleoenvironmental studies in China combining the terrestrial and marine realms. The first important results from the leg include the establishment of deep-sea stratigraphic sequences in the SCS, and the exploration of changing climate cyclicity since the beginning of the Neogene, namely:

(1) Set up of the best deep-sea stratigraphic sections in the Western Pacific, including i) a 23 Ma isotope sequence near Dongsha without splicing which is unique

in the global ocean, ii) one of the four 5 Ma sequences worldwide with highest time resolution from near Nansha, and iii) physical property sequences on decadal time scale. This offers the first set of high-quality marine records for paleoenvironmental studies in the Asian-Pacific region.

(2) A number of global events have been detected in the SCS records, such as the Antarctic ice-cap expansions in the Miocene, and the Arctic ice-cap formation. All these are beneficial to international calibration of environmental events in and beyond China. The regional and local events found in the SCS include a deep-sea environment already existing in the beginning of seafloor spreading at ~32 Ma and a major tectonic transformation in the late Oligocene (27—23 Ma) which will be discussed in our next papers.

(3) The late Cenozoic continuous oxygen isotope record from the SCS has been utilized to systematically explore the evolution of climate cycles driven by orbital forcing. Eccentricity cycles of 2000 ka, 400 ka and 100 ka vary significantly in amplitude over the Neogene-Quaternary periods, suggesting that the climate system changes its way of response to the orbital cycles with the growth of polar ice-sheets. The prevalent understanding of the Milankovitch cycles, based primarily on late Quaternary records, represents a specific case after the Arctic ice-sheet expansion.

**Acknowledgements** The present paper is the first of three summary reports of the ODP leg to the SCS. This work was supported by the National Natural Science Foundation of China (Grant No. 49999560) and the National Key Basic Research Special Fund (Grant G2000078500). This research used samples and data provided by the ODP, which is sponsored by the U.S. National Science Foundation and participating countries under management of Joint Oceanographic Institutions, Inc.

## References

- Wang, P., Prell, W., Blum, P. et al., Proceedings of Ocean Drilling Program, Initial Reports, Volume 184, College Station: Ocean Drilling Program, 2000, 77.
- Zhao, Q., Jian, Z., Wang, J. et al., Neogene oxygen isotopic stratigraphy, ODP Site 1148, northern South China Sea, Science in China, Ser. D, 2001, 44(10): 934—942.
- Zhao, Q., Wang, P., Cheng, X. et al., A record of Miocene carbon excursions in the South China Sea, Science in China, Ser. D, 2001, 44(10): 943—951.
- Tian, J., Wang, P., Cheng, X. et al., Astronomically tuned Pliocene benthic  $\delta^{18}\text{O}$  record from South China Sea and Atlantic-Pacific comparison, Earth and Planetary Science Letters, 2002, 203: 1015—1029.
- Wang, P., Tian, J., Cheng, X., Transition of Quaternary glacial cyclicity in deep-sea records at Nansha, the South China Sea, Science in China, Ser. D, 2001, 44(10): 926—933.
- Shao, L., Li, X., Wei, G. et al., Provenance of a prominent sediment drift on the northern slope of the South China Sea, Science in China, Ser. D, 2001, 44(10): 919—125.
- Li, B., Jian, Z., Evolution of planktonic foraminifera and thermocline in the southern South China Sea since 12 Ma (OSP-184, Site 1143), Science in China, Ser. D, 2001, 44(10): 889—896.
- Shackleton, N. J., Hall, M. A., Pate, D., Pliocene stable isotope stratigraphy of Site 846 (eds. Pisias, G., Mayer, L. A., Janecek, T. R. et al.), Proc. ODP Sci. Results, 1995, 138: 337—355.
- Mix, A., Pisias, N. G., Rugh, W. et al., Benthic foraminifer stable isotope record from Site 849 (0—5 Ma): Local and global climate changes (eds. Pisias, N. G., Mayer, L. A., Janecek, T. R. et al.), Proc. ODP Sci Results, 1995, 138: 371—412.
- Tiedemann, R., Sarnthein, M., Shackleton, N. J., Astronomic time-scale for the Pliocene Atlantic  $\delta^{18}\text{O}$  and dust flux records from Ocean Drilling Program Site 659, Paleoceanography, 1994, 9: 619—638.
- Savin, S. M., Douglas, R. G., Keller, G. et al., Miocene benthic foraminifer isotope records: A synthesis, Marine Micropaleontology, 1981, 6: 423—450.
- Woodruff, F., Savin, S. M., Mid-Miocene isotope stratigraphy in the deep sea: High-resolution correlations, paleoclimatic cycles, and sediment preservation, Paleoceanography, 1991, 6(6): 755—806.
- Hodell, D. A., Vayavandana, A., Middle Miocene paleoceanography of the western equatorial Pacific (DSDP site 289) and the evolution of *Globorotalia* (*Fohsella*), Marine Micropaleontology, 1993, 22: 279—310.
- Kennett, J. P., Miocene to early Pliocene oxygen and carbon stratigraphy of the Southwest Pacific, DSDP Leg 90, Init. Repts DSDP 90, pt.2, 1986, 1383—1411.
- Flower, B. P., Kennett, J. P., Middle Miocene ocean-climate transition: High-resolution oxygen and carbon isotopic records from Deep Sea Drilling Project Site 588A, Southwest Pacific, Paleoceanography, 1993, 8(6): 811—843.
- Woodruff, F., Savin, S. M., Abel, L., Miocene benthic foraminifer oxygen and carbon isotopes, Site 709, Indian Ocean. Proc. ODP, Sci. Res., 1990, 115: 519—528.
- Miller, K. G., Wright, J. D., Fairbanks, R. G., Unlocking the ice house: Oligocene-Miocene oxygen isotopes, eustasy, and margin erosion, Journal of Geophysical Research, 1991, 96(B4): 6829—6848.
- Wright, J. D., Miller, K. G., Fairbanks, R. G., Early and middle Miocene stable isotopes: Implications for deepwater circulation and climate, Paleoceanography, 1992, 7(3): 357—389.
- Zachos, J. S., Pagani, M., Sloan, L. et al., Trends, rhythms, and aberrations in global climate 65 Ma to present, Science, 2001A, 292: 686—693.
- Flower, B. P., Kennett, J. P., Middle Miocene paleoceanography in the Southwest Pacific: Relations with East Antarctic Ice Sheet development, Paleoceanography, 1995, 10(6): 1095—1112.
- Mutti, M., Bulk  $\delta^{18}\text{O}$  and  $\delta^{13}\text{C}$  records from Site 999, Colombia Basin, and Site 1000, Nicaraguan Rise (late Oligocene to middle Miocene): Diagenesis, Link to sediment parameters, and paleoceanography, Proc. ODP, Sci. Res., 2000, 165: 275—283.
- Billups, K., Channell, J. E. T., Zachos, J., Late Oligocene to early Miocene geochronology and paleoceanography from the subantarctic South Atlantic, Paleoceanography, 2002, 17(1): 4-1—4-10.
- Jian, Z., Cheng, X., Zhao, Q. et al., Oxygen isotope stratigraphy and events in the northern South China Sea during the last 6 million years, Science in China, Ser. D, 2001, 44(10): 952—960.
- Jian, Z., Zhao, Q., Cheng, X. et al., Pliocene-Pleistocene stable isotope and paleoceanographic changes in the northern South China Sea. Palaeogeography, Palaeoclimatology, Palaeoecology, 2003, in press.
- Kennett, J. P., Hodell, D. A., Evidence for relative climatic stability of Antarctica during the Early Pliocene: a marine perspective, Geografiska Annaler, 1993, 75A(4): 205—220.

26. Hodell, D. A., Woodruff, F., Variations in the strontium isotopic ratio of seawater during the Miocene: Stratigraphic and geochemical implications, *Paleoceanography*, 1994, 9(3): 405—426.
27. Flower, B. P., Zachos, J. C., Paul, H., Milankovitch-scale climate variability recorded near the Oligocene/Miocene boundary, *Proc. ODP, Sci Res.*, 1997, 154: 433—439.
28. Vincent, E., Berger, W. H., Carbon dioxide and polar cooling in the Miocene: the Monterey hypothesis, *Geophys. Monogr.*, 1985, 32: 455—468.
29. Roth, J. M., Droxler, A. W., Kameo, K., The Caribbean carbonate crash at the middle to late Miocene transition: Linkage to the establishment of the modern global ocean conveyor, *Proc. ODP, Sci. Res.*, 2000, 165: 249—273.
30. Berger, W. H., Jansen, E., Mid-Pleistocene climate shift—The Nansen connection, *Geophysical Monograph*, 1994, 84: 295—311.
31. Raymo, M. E., Oppo, D. W., Curry, W., The mid-Pleistocene climate transition: A deep sea carbon isotopic perspective, *Paleoceanography*, 1997, 12(4): 546—559.
32. Mudelsee, M., Stattegger, K., Exploring the structure of the mid-Pleistocene revolution with advanced methods of time-series analysis, *Geol Rundsch.*, 1997, 86: 499—511.
33. Schmieder, F., von Dobeneck, T., Bleil, U., The Mid-Pleistocene climate transition as documented in the deep South Atlantic Ocean: initiation, intermstate and terminal event, *Earth and Planetary Science Letters*, 2000, 179: 539—549.
34. Rutherford, S., D'Hondt, S., Early onset and tropical forcing of 100,000-year Pleistocene glacial cycles, *Nature*, 2000, 408: 72—75.
35. Clemens, S., Tiedemann, R., Eccentricity forcing of Pliocene-Early Pleistocene climate revealed in a marine oxygen-isotope record, *Nature*, 1997, 385: 801—804.
36. Paul, H. A., Zachos, J. C., Flower, B. P. et al., Orbitally induced climate and geochemical variability across the Oligocene/Miocene boundary, *Paleoceanography*, 2000, 15(5): 471—485.
37. Zachos, J. S., Shackleton, N. J., Revenaugh, J. S. et al., Flower BP. Climate response to orbital forcing across the Oligocene-Miocene boundary, *Science*, 2001, 292: 274—278.
38. Turco, E., Hilgen, F. J., Lourens, L. J. et al., Punctuated evolution of global cooling during the late Middle to early Late Miocene: High-resolution planktonic foraminiferal and oxygen isotope records from the Mediterranean, *Paleoceanography*, 2001, 16(4): 405—423.
39. Van Couvering, J. A., Castradori, D., Cita, M. B. et al., The base of the Zanclean Stage and of the Pliocene Series, *Episodes*, 2000, 23(3): 179—187.
40. Ruddiman, W. F., *Earth's Climate: Past and Future*, New York: Freeman W H & Co, 2001, 465.
41. Short, D. A., Mengel, J. G., Crowley, T. J. et al., North GR. Filtering of Milankovitch cycles by Earth's geography, *Quaternary Research*, 1991, 35: 157—173.
42. Olsen, P. E., Kent, D. V., Milankovitch climate forcing in the tropics of Pangaea during the Late Triassic, *Palaeo Palaeo Palaeo*, 1996, 122: 1—26.
43. Matthews, R. K., Frohlich, C., Maximum flooding surfaces and sequence boundaries: Comparisons between observations and orbital forcing in the Cretaceous and Jurassic (65—190 Ma), *GeoArabia, Middle East Petroleum Geoscientists*, 2002, 7: 503—538.
44. Imbrie, J., Berger, A., Boyle, E. A. et al., On the structure and origin of major glaciation cycles, 2, the 100,000-year cycle, *Paleoceanography*, 1993, 8: 699—735.

(Received April 1, 2003; accepted July 28, 2003)